Electronic Supporting Information (ESI)

Oxygen-Vacancy–Enabled Charge Separation in Distorted Orthorhombic $YFeO_3$

Md. Sobuj Hossain and M. A. Basith*

Nanotechnology Research Laboratory, Department of Physics,

Bangladesh University of Engineering and Technology, Dhaka-1000, Bangladesh..

*Corresponding author(s). E-mail: mabasith@phy.buet.ac.bd

Synthesis of nanoporous $YFeO_3$:

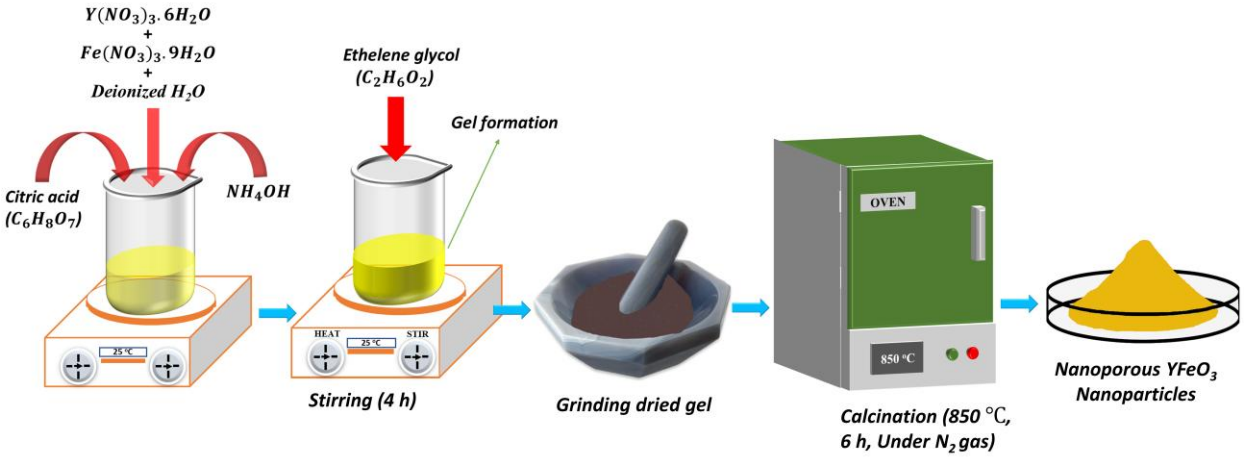

Fig. S1 *Schematic representation of the sol–gel synthesis route of nanoporous $YFeO_3$ nanoparticles.*

Nanoporous $YFeO_3$ powders were synthesized via a citrate–ethylene glycol-assisted sol–gel auto-combustion route[1], as schematically shown in Fig. S1. Stoichiometric amounts of yttrium nitrate hexahydrate [$Y(NO_3)_3 \cdot 6H_2O$, 99.8%, Sigma-Aldrich] and iron nitrate nonahydrate [$Fe(NO_3)_3 \cdot 9H_2O$, 99.8%, Sigma-Aldrich] were separately dissolved in 100 mL deionized water and stirred at room temperature (27 °C) for 30 min before mixing. Citric acid (Y:Fe:CA = 1:1:2)

was introduced as a chelating agent, and the pH was adjusted to 7 using 2.0 M NH_4OH (added dropwise at 0.5 mL min^{-1}). Ethylene glycol (EG), added in an EG:CA molar ratio of 4:1, served as a polymeric cross-linker to facilitate gel formation and molecular-level homogeneity. The sol was aged for 4 h to enable network development and then gradually heated to 200 °C to initiate auto-combustion, producing a foamed precursor. This intermediate was dried and finely ground in an agate mortar. Calcination was conducted at 850 °C for 3 h in a flowing N_2 atmosphere (5 °C min^{-1} ramp) using a loosely covered alumina crucible. The inert atmosphere suppressed over-oxidation and enabled the formation of phase-pure, compositionally uniform $YFeO_3$ with a mesoporous structure. During gel evolution, ethylene glycol reacts with the metal–citrate complex to form a cross-linked polymeric matrix. Upon thermal treatment, the decomposition of this organic network generates H_2O and CO_2 gases, which escape and leave voids between particles. The constrained shrinkage during crystallization under N_2 preserves this porosity. The resulting nanostructured architecture enhances the photocatalyst's light-harvesting capacity, surface reactivity, and mass transport—key attributes for efficient photocatalytic degradation of pollutants.

Electrochemical cell setup for Mott-Schottky and photoelechtrochemical analysis

A three-electrode and a symmetric two-electrode systems was employed in an eutral 0.5 M Na_2SO_4 aqueous electrolyte was to evaluate the electrochemical behavior of $YFeO_3$ nanoparticles (Fig. S2). The three-electrode setup, designed for Mott–Schottky analysis, incorporated a platinum wire counter electrode and an *Ag/AgCl* (3 M KCl) reference electrode. The working electrode was prepared by dispersing 90 mg (90 wt%) of as-synthesized nanoporous $YFeO_3$ and 10 mg (10 wt%) of polyvinylidene fluoride (PVDF) in 180 µL of N-methyl-2-pyrrolidone (NMP). The resulting slurry was sonicated for 2 h to ensure homogeneity and then coated onto a graphite rod (active area: 0.28 cm^2), followed by drying at 60 °C for 12 h.

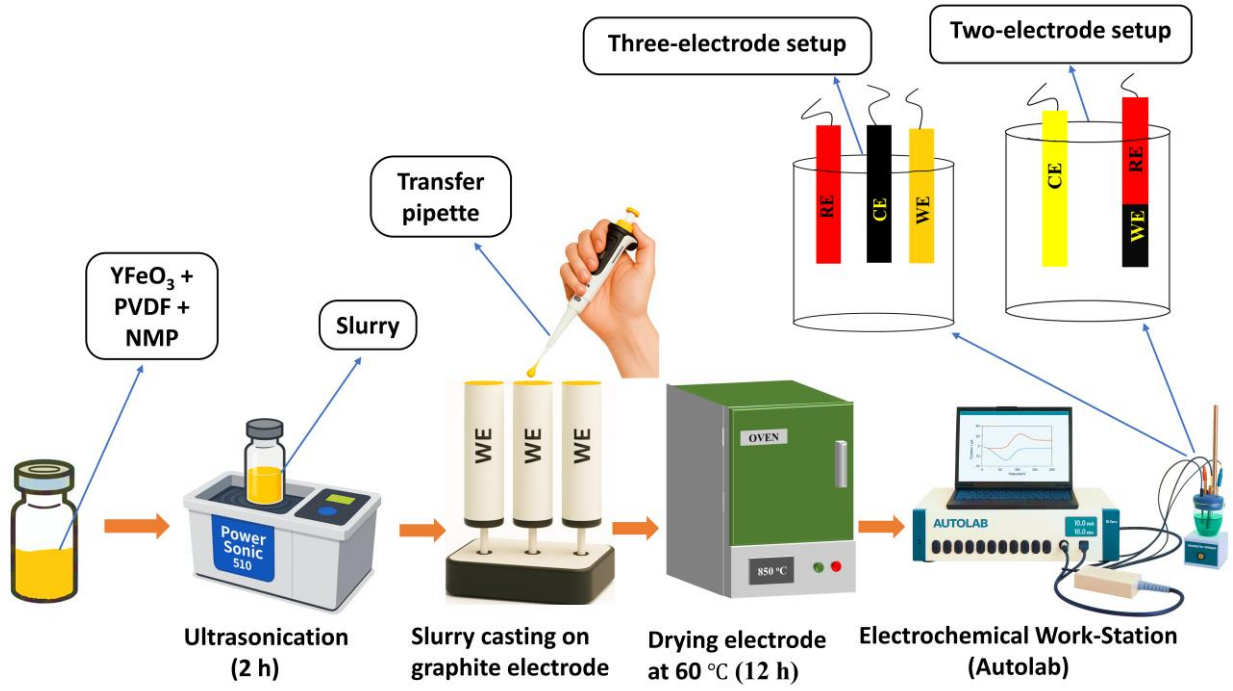

Fig. S2 *Schematic illustration of the preparation of electrode slurry and the configuration of the electrochemical setup for Mott–Schottky and photoelectrochemical analysis.*

For photoelectrochemical testing, a symmetric two-electrode configuration was fabricated by depositing equal amounts of the same $YFeO_3$–PVDF slurry onto two identical graphite rods under identical conditions. These modified rods served as both the anode and cathode in the symmetric device. This configuration enabled assessment of photocurrent response and interfacial charge dynamics under visible-light irradiation.

Table S1 *Crystallographic parameters of the as-synthesized porous $YFeO_3$ nanoparticles before and after 4 cycles of photocatalysis obtained after Rietveld refinement. Analysis of the XRD data suggests that this material maintained its structural integrity without undergoing any phase transformation making our synthesized nanoparticles a reliable catalyst for photocatalytic wastewater treatment.*

Parameters	**Before**	**After 4 cycles of photocatalysis**
Crystallographic phase	Orthorhombic	Orthorhombic
Space group	$Pnma$	$Pnma$
a (Å)	5.621191	5.62124
b (Å)	7.643383	7.64332
c (Å)	5.308568	5.30815
$\alpha = \beta = \gamma$ (degree)	90	90
Crystallinity (%)	84 %	77.06 %
R_p	4.6%	3.5%
R_{wp}	6.5%	6.92%
Goodness of fit, χ^2	1.41	2.39

Table S2 Bond lengths, Fe–O–Fe bond angles, and octahedral tilt angles of $YFeO_3$ (space group Pnma). Fractional coordinates are given with respect to a, b, and c. O1 and O2 denote apical (4c) and equatorial (8d) oxygens, respectively. Tilt angles are defined as $\theta = (180^\circ - \angle Fe{-}O{-}Fe)/2$, with α from O1 (antiphase) and γ from O2 (in-phase).

Bond Geometry			
Bond length (°)	Bond Angle(Å)	Tilt angle (°)	Average tilt angle (°)
Fe-O1= 2.0254 Å	Fe-O1-Fe = 141.27°	$\alpha = 19.365$ (Antiphase)	18.8 ± 0.3
Fe-O2= 2.0144 Å	Fe-O2-Fe = 143.48°	$\gamma = 18.26$ (In phase)	
Fe-O2= 2.0563 Å			

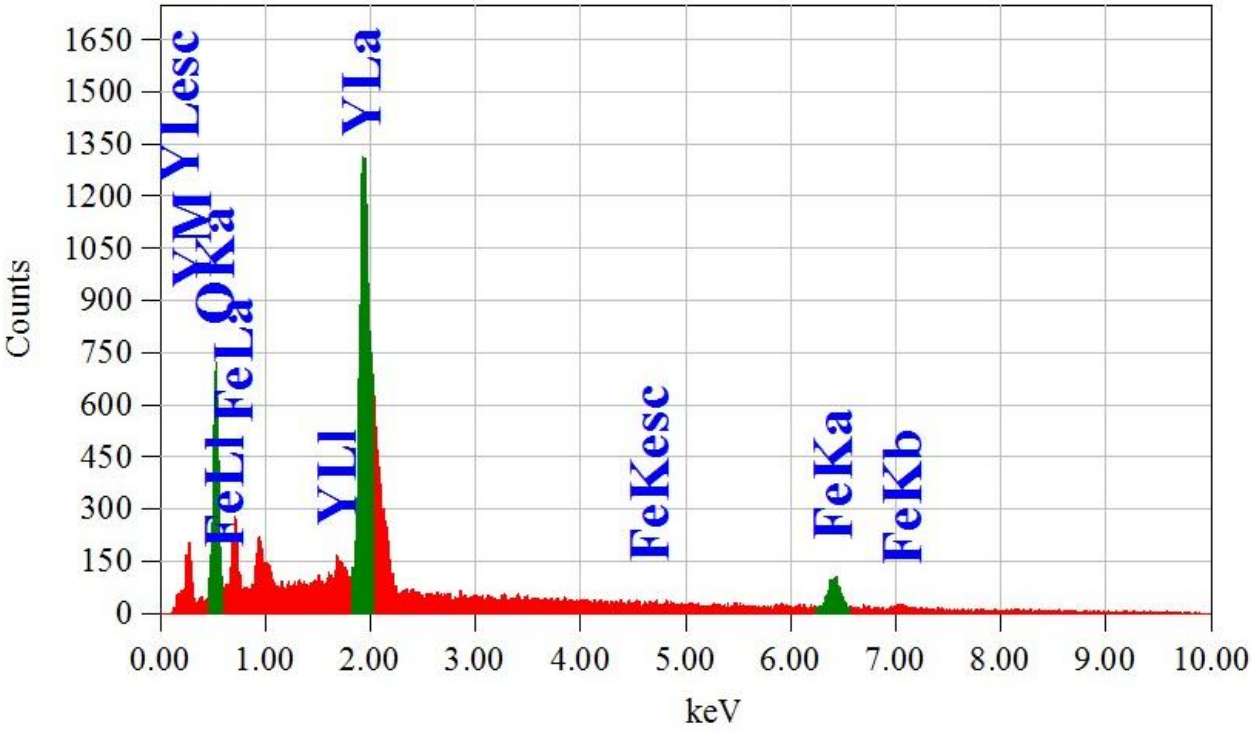

Fig. S3 *Energy-dispersive x-ray (EDX) spectrum confirming the elemental composition of $YFeO_3$ nanoparticles, indicating the presence of Y, Fe, and O.*

Table S3 *Elemental composition of $YFeO_3$ nanoparticles determined by EDX analysis. The measured mass and atomic percentages agree with theoretical values, confirming the successful formation of the $YFeO_3$ phase.*

Elements	**Mass (%) (theoretical)**	**Mass (%) (experimental)**	**Atomic (%) (theoretical)**	**Atomic (%) (experimental)**
Y	46.13	50.69	20	25.08
Fe	28.97	30.92	20	24.36
O	24.90	18.39	60	50.56

Table S4 *X-ray photoelectron spectroscopy (XPS) peak assignments and fitted binding energies for $YFeO_3$ nanoparticles. Listed are the element, core level, component peak, and binding energy (eV).*

Element	Orbital	Peaks	Binding energy (eV)	Percentage of ion and satellite peaks
Y	3d	$3d_{3/2}$ (Y^{3+})	159.74	14.9
			158.7	31.3
		$3d_{5/2}$ (Y^{3+})	157.84	5.8
			156.82	48
	3p	$3p_{1/2}$ (Y^{3+})	312.09	35.3
		$3p_{3/2}$ (Y^{3+})	300.21	64.7
Fe	2p	$2p_{1/2}$ (Y^{3+})	725.35	13.7
		$2p_{1/2}$ (Y^{2+})	723.73	13.2
		$2p_{3/2}$ (Y^{3+})	711.60	39.7
		$2p_{3/2}$ (Y^{2+})	710.16	28.3
		Satellite	732.7	2.7
			718.60	2.4
O	1s	O^{2-}	529.3	59.1
		O_{vacan}	531.39	39
		OH^-	532.88	1.9

Experimental setup for photocatalytic degradation of pollutants from water

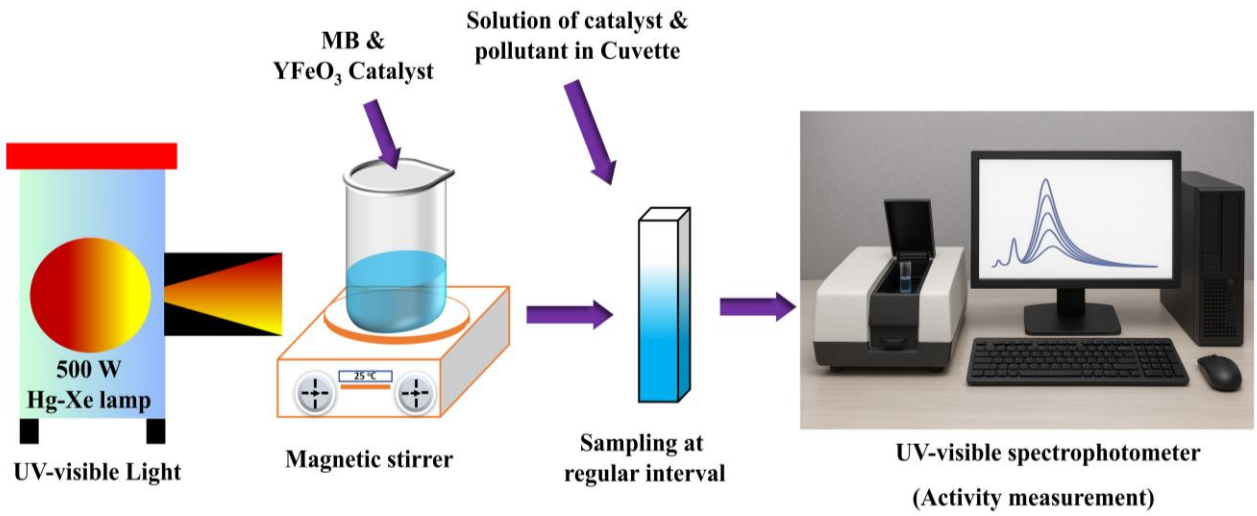

Fig. S4 *Schematically representation of photocatalytic reactor setup for the pollutant (MB) degradation experiments. Irradiation power density was 100 mW* cm^{-2}.

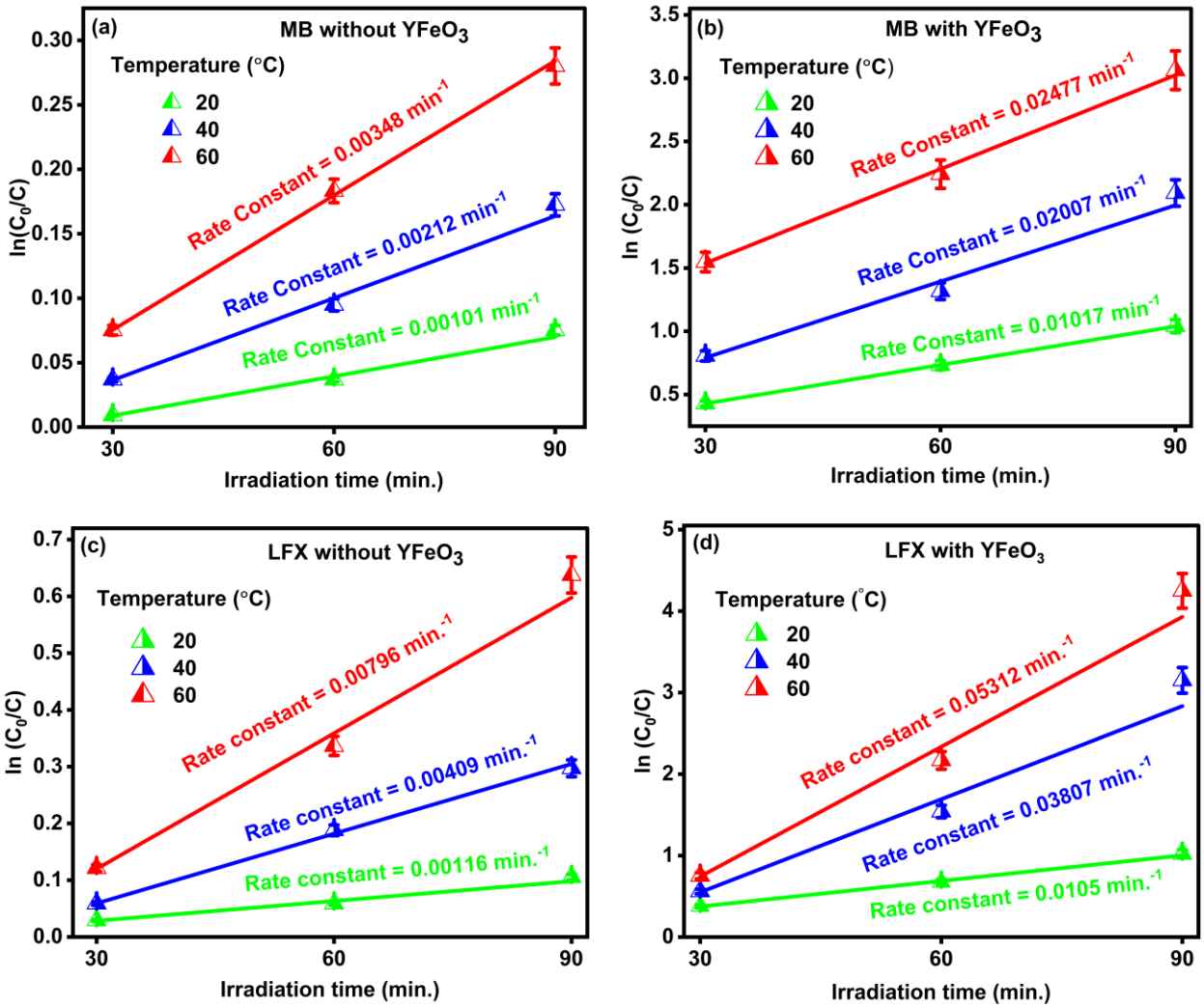

Fig. S5 *Activation energy measurement of MB and LFX. (a, c) represent the pseudo-first-order kinetics of MB without and with the presence of $YFeO_3$ photocatalyst, respectively. And (c,d)) represent the pseudo-first-order kinetics of LFX without and with the presence of $YFeO_3$ photocatalyst, respectively. These results indicate the true photocatalytic activity of $YFeO_3$ nanoparticles.*

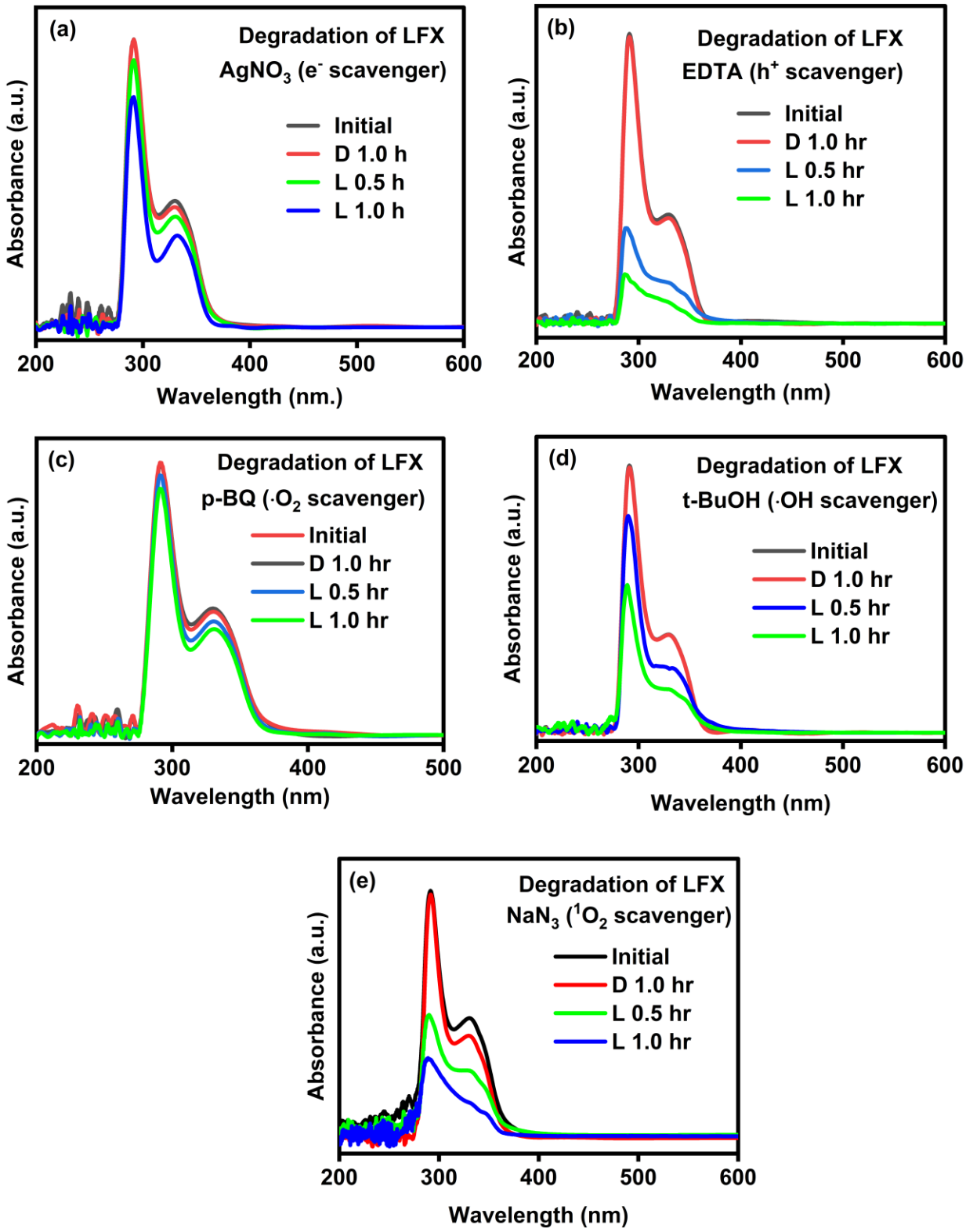

Fig. S6 *Photocatalytic degradation of LFX in the presence of $YFeO_3$ photocatalyst and (a) $AgNO_3$, (b) EDTA 2Na, (c) p-BQ, (d) t-BuOH and NaN_3 trapping reagents.*

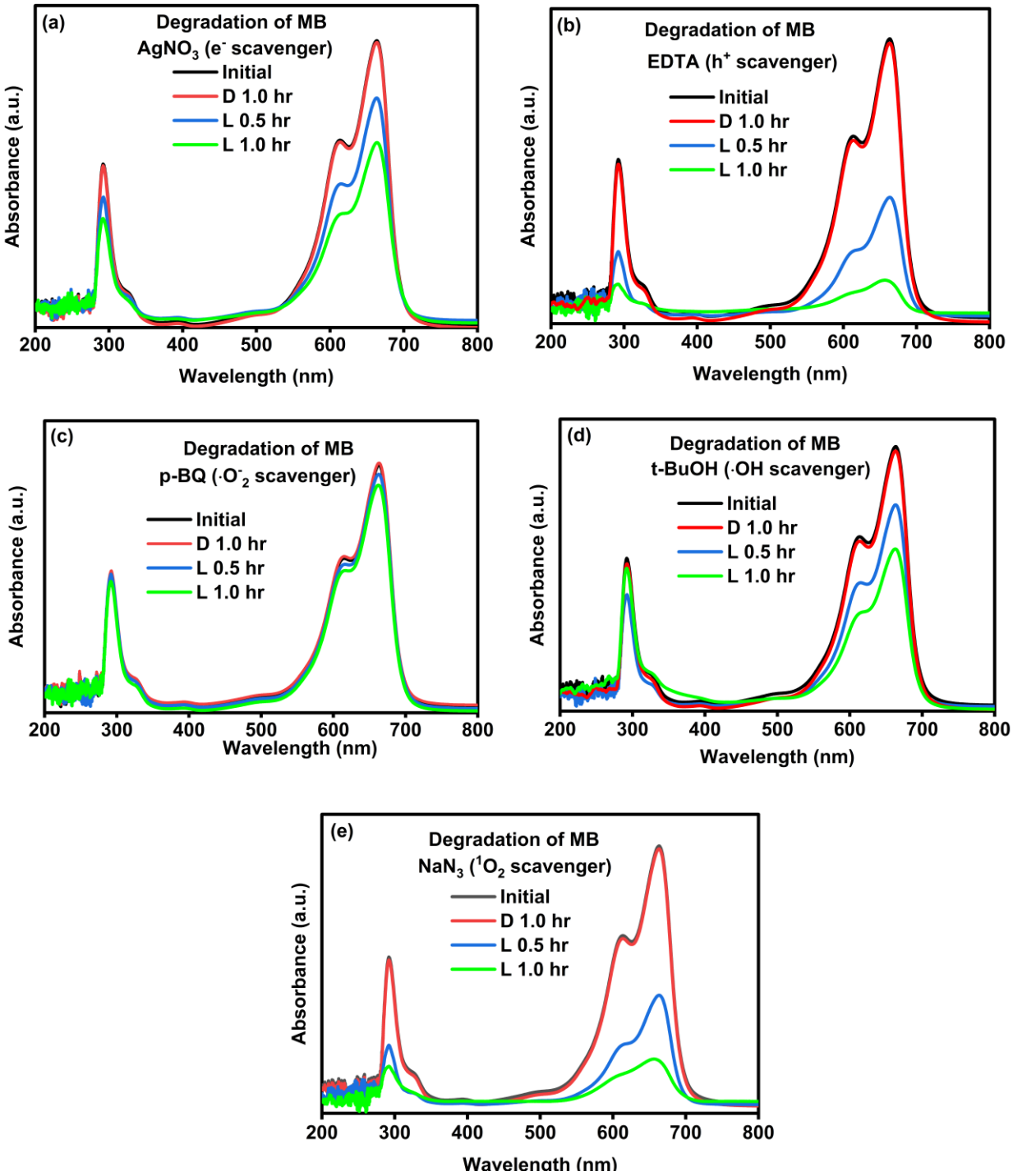

Fig. S7 *Photocatalytic degradation of MB in the presence of $YFeO_3$ photocatalyst and (a) $AgNO_3$, (b) EDTA 2Na, (c) p-BQ, (d) t-BuOH and NaN_3 trapping reagents.*

Table S5 *Equivalent-circuit fitting parameters obtained from electrochemical impedance spectroscopy (EIS) measurements of the $YFeO_3$ symmetric cell under dark and illuminated conditions, using the circuit $R_1(CPE_1(R_2(CPE_2R_3)(CPE_3(R_4W))))$. R_1 (denoted as Rs) represents the uncompensated solution resistance. R_2 and CPE_1 correspond to bulk (grain interior) transport in $YFeO_3$, while R_3 and CPE_2 describe grain-boundary/surface trap processes. R_4 (denoted as R_{ct}) and CPE_3 are associated with*

Parameter	Physical Meaning	Value (Dark)	Value (Light)
R_1 (R_s)	Electrolyte resistance	26.39 Ω	14.13 Ω
R_2	Bulk resistance	32 Ω	30.5 Ω
R_3	Grain boundary resistance	68.4 Ω	55.2 Ω
R_4 (R_{ct})	Charge transfer resistance	104 Ω	88.2 Ω
CPE_1	Bulk CPE	8.6×10^{-4} S·s^n	9.4×10^{-4} S·s^n
n_1	Bulk ideality	0.95	0.96
CPE_2	Grain boundary CPE	3.8×10^{-4} S·s^n	4.6×10^{-4} S·s^n
n_2	GB ideality	0.89	0.91
CPE_3	Double-layer CPE	1.2×10^{-4} S·s^n	1.9×10^{-4} S·s^n
n_3	Interface ideality	0.84	0.87
W	Warburg diffusion	215 Ω·s$^{-0.5}$	165 Ω·s$^{-0.5}$
χ^2 error	Fitting	1.62×10^{-5}	4.55×10^{-6}

Table S6 *A brief review of the pollutant degrading capabilities exhibited by $YFeO_3$ nanoparticles photocatalysts compared to other commonly used photocatalysts in recent investigations. This table suggests that our synthesized $YFeO_3$ nanoparticles photocatalyst exhibited superior photocatalytic degradation performances on both industrial dye and pharmaceutical antibiotics surpassing or comparable with the other photocatalysts.*

Perovskite	Light source	Synthesis method	Pollutant	Pollutant conc.	Catalyst conc.	Irradiation time (min.)	Degradation (%)	Ref.
$BiFeO_3$	500 W Hg-Xe	Solgel	Ciprofloxacin	10 mg L^{-1}	0.8 g L^{-1}	240	42	[2]
			Levofloxacin				46	
$SmFeO_3$	300 W	Sol-gel	Rhodamine B	20 mg L^{-1}	1.5 g L^{-1}	300	45	[3]
$LaFeO_3$	200 W Xe	Sol-gel	Rhodamine B	5 mg L^{-1}	1.0 g L^{-1}	180	67.4	[4]
$SrFeO_3$	150 W Xe	Combustion	Rhodamine B	5 mg L^{-1}	0.3 g L^{-1}		43	[5]
$BiFeO_3$	-	Sol-gel	Ciprofloxacin	10 mg L^{-1}	2 g L^{-1}	60	<20	[6]
$DyFeO_3$	500 W Hg-Xe	Sol-gel	Levofloxacin	10 mg L^{-1}	0.4 g L^{-1}	240	88.38	[1]
			Rhodamine B	12 mg L^{-1}	0.8 g L^{-1}		85.9	
$LuFeO_3$	200 W xenon lamp	Polyacrylamide gel route	Rhodamine B	2 mg L^{-1}	1.0 g L^{-1}	360	51	7
$YFeO_3$ Orthoferrite (nanoporous)	500 W Hg-Xe	Sol-gel	Methylene blue	12 mg L^{-1}	0.4 g L^{-1}	240	82	This work
			Levofloxacin	10 mg L^{-1}			88.43	

Apparent Quantum Yield (AQY) calculation

Step 1: Degraded pollutant molecule calculation

$$\text{Total molecules} = \text{No. of moles in a solution} \times \text{Avogadro's number}$$

$$\text{Weight} = \text{Concentration} \times \text{Volume}$$

$$\text{Moles} = \text{Molecular weight}/\ \text{Weight}$$

$$\text{Degraded molecules} = \text{Total no. of pollutant molecules} \times (\text{Degradation percentage})/100$$

With Photocatalyst			
Detail	Unit	MB (YFO)	LFX (YFO)
Pollutant solution	L	0.05	0.05
Pollutant concentration	g/L	0.012	0.01
Pollutant weight in solution	g	0.0006	0.0005
Molecular weight	g/mol	319.85	361.37
No. of moles in a solution	mol	1.87×10^{-6}	1.38×10^{-6}
No. of molecules in a mole	molecules/mol	6.023×10^{23}	6.023×10^{23}
Total no. of pollutant molecules	molecules	1.12×10^{18}	8.31×10^{17}
Degradation percentage	%	82	88.43
No. of degraded molecules	molecules	9.184×10^{17}	7.34×10^{17}

Without Photocatalyst			
Details	Unit	MB	LFX
Pollutant solution	L	0.05	0.05
Pollutant concentration	g/L	0.012	0.01
Pollutant weight in solution	g	0.0006	0.0005
Molecular weight	g/mol	319.85	361.37
No. of moles in a solution	mol	1.87×10^{-6}	1.38×10^{-6}
No. of molecules in a mole	molecules/mol	6.023×10^{23}	6.023×10^{23}
Total no. of pollutant molecules	molecules	1.12×10^{18}	8.31×10^{17}
Degradation percentage	%	10	12
No. of degraded molecules	molecules	1.12×10^{17}	9.97×10^{16}

Step 2: Photon energy calculation

Wavelength of light, λ = 440 nm = 440 × 10^{-9} m

Energy of one photon, $E = \frac{hc}{\lambda} = \frac{6.6\times10^{-34}\times3\times10^{8}}{440\times10-9} = 4.50\ \times 10^{-19}\ Joules$

The total energy of light falling per second per unit area is

$$E_{Total} = 100\ mW\ cm^{-2} = \ 100\ \times 10^{-3} \times 10^{4} W\ m^{-2} = \ 1000\ W\ m^{-2}$$

Number of Photon = $\frac{E_{Total}}{\mathrm{E}} = \frac{1000}{4.50\times10^{-19}} = 2.22 \times 10^{21}$

Area of exposed solution = $\frac{2\pi rl}{2} = \pi rl$

Total number of Photon falling on the solution (Number of incident Photon) = Number of Photon × Area of exposed solution

Apparent Quantum Yield (AQY) = $\frac{Number\ of\ degraded\ molecule}{Number\ of\ incident\ photon} \times 100$

Without catalyst				
Irradiation time (min.)	Area of exposed solution (m^2)	Number of incident photon	Apparent Quantum Yield (%) in MB	Apparent Quantum Yield (%) in LFX
240	0.001007	2.24×10^{18}	5	4.45

With catalyst				
Irradiation time (min.)	Area of exposed solution (m^2)	Number of incident photon	Apparent Quantum Yield (%) in MB ($YFeO_3$)	Apparent Quantum Yield (%) in LFX ($YFeO_3$)
240	0.001007	2.24×10^{18}	41	32.81

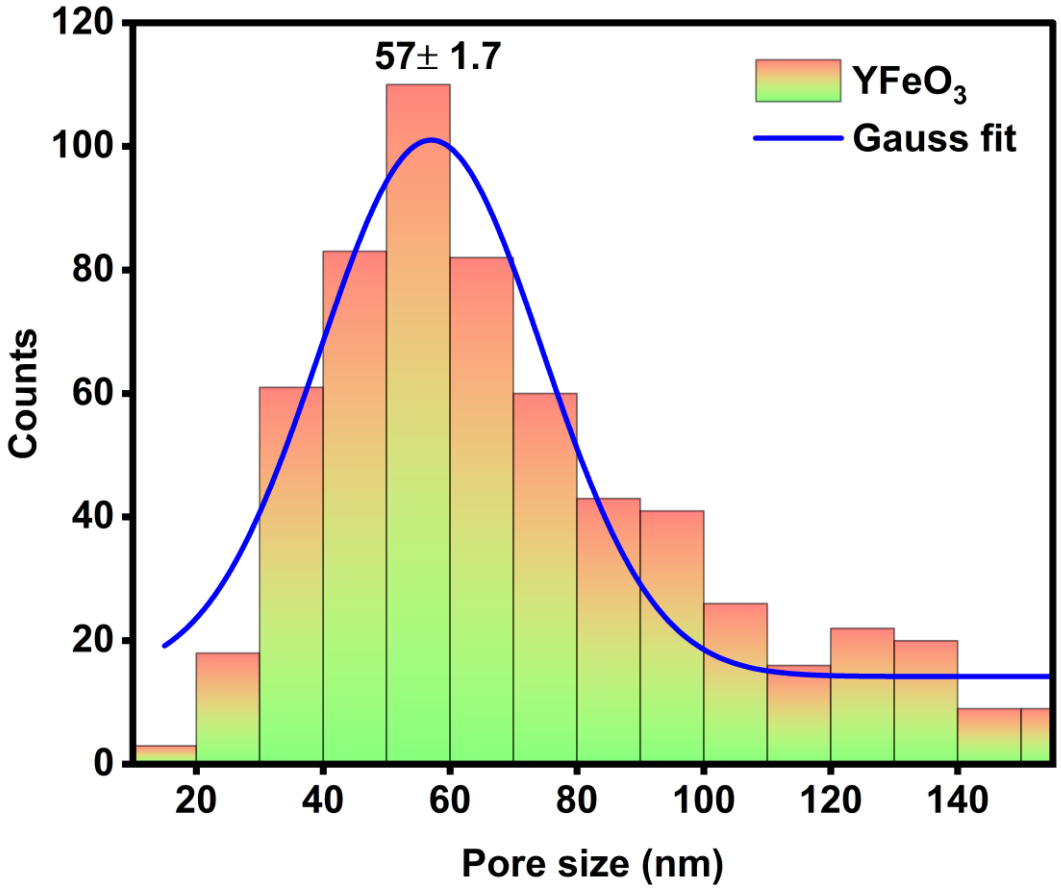

Fig. S8 *Pore size distribution from FESEM image of $YFeO_3$ after 5 consecutive photocatalysis degradation cycles.*

References:

1. Tarek, F. Yasmeen and M. A. Basith, J. Mater. Chem. A, 2024, 12, 25475–25490.
2. T. V. Rozario, F. Sharmin, S. Shamim and M. Basith, *Ceram. Int.,* 2024, 50, 3606–3617.
3. Z. Behzadifard, Z. Shariatinia and M. Jourshabani, *J. Mol. Liq.*, 2018, 262, 533–548.
4. S. Guan, R. Li, X. Sun, T. Xian and H. Yang, *Mater. Technol.*, 2021, 36, 603–615.
5. M. N. Ha, L. Wang and Z. Zhao, *Res. Chem. Intermediate*, 2019, 45, 1493–1508.
6. C. Wang, S. Gao, J. Zhu, X. Xia, M. Wang and Y. Xiong, *J. Environ. Sci.*, 2021, 99, 249–259.
7. M. Zhou, H. Yang, T. Xian and C. R. Zhang, *Phys. Scr.*, 2015, 90, 085808.